Surface Science 605 (2011) L51–L55

Contents lists available at ScienceDirect

Surface Science

journal homepage: www.elsevier.com/ locate/susc

Surface Science Letters

The (2×2) reconstructions on the $SrTiO_3$ (001) surface: A combined scanning tunneling microscopy and density functional theory study

Yuyuan Lin [a,*], Andres E. Becerra-Toledo [a], Fabien Silly [b], Kenneth R. Poeppelmeier [c], Martin R. Castell [d], Laurence D. Marks [a]

[a] Department of Materials Science and Engineering, Northwestern University, IL 60208, USA
[b] CEA, IRAMIS, SPCSI, F-91191 Gif-sur-Yvette, France
[c] Department of Chemistry, Northwestern University, Evanston, IL 60208, USA
[d] Department of Materials, University of Oxford, Parks Road, Oxford, OX1 3PH, UK

ARTICLE INFO

Article history:
Received 16 November 2010
Accepted 1 June 2011
Available online 12 June 2011

Keywords:
Density functional theory
Scanning tunneling microscopy
Surface reconstruction
Simulation
Strontium titanate
Surface structure

ABSTRACT

Scanning tunneling microscopy study showed that the (2×2) reconstruction on the (001) surface of $SrTiO_3$ should have a surface structure with a 4-fold symmetry. The previously proposed solution for the (2×2) reconstruction with the p2gm symmetry only has a 2-fold symmetry. In this study density functional theory study was carried out to propose a possible surface structure with the p4mm surface symmetry which matches the scanning tunneling microscopy images and suggests that two different (2×2) surface structures exist. The formation of the (2×2) reconstruction with the p4mm symmetry may be due to the kinetics as it has slightly higher surface energy than the one with the p2gm symmetry.

The surface structures of strontium titanate ($SrTiO_3$) have attracted much interest because of applications ranging from photo-catalysis [1] to thin film and nanostructure growth [2–4], as well as the fact that $SrTiO_3$ is the archetypal perovskite, so understanding the surface structures will help understand other, similar materials. For the $SrTiO_3$ (001) surface, a number of reconstructions have been observed including (1×1) [5], (2×1) [6–8], (2×2) [5,9–15], c(4×2) [6,16,17], c(4×4) [6], (4×4) [18], c(6×2) [16,19], $(\sqrt{5}\times\sqrt{5})R26.6°$ [20–23] and $(\sqrt{13}\times\sqrt{13})R33.7°$ [24,25] using various surface sensitive techniques. The $SrTiO_3$ (001) surface can also form TiO_x-rich nanostructures that order into (n×2), (6×8), or (7×4) surface patterns [26–31]. Among the reconstructions on the (001) surface, only the c(4×2), (2×1), one form of the (2×2) [32,33], c(6×2) and $(\sqrt{13}\times\sqrt{13})R33.7°$ [25] reconstructions have been structurally solved, while the other reconstructions are still unclear. In the present paper, density functional theory (DFT) and scanning tunneling microscopy (STM) studies were carried out to understand a square (2×2) reconstructed structure on the $SrTiO_3$ (001) surface, which has a 4-fold surface symmetry and is different from the previously solved $SrTiO_3$(001)-(2×2) (which is rectangular with p2gm symmetry).

The (2×2) reconstruction on the $SrTiO_3$ (001) surface was first reported by Cord et al., who used low-energy electron diffraction (LEED) and annealed the sample in an oxygen-rich vacuum; no structural model was proposed [5]. A further LEED study of the (2×2) surface was reported in 1990 and attributed, probably erroneously, to the influence of Ca impurities [9], as later papers by the same authors show a (2×2) reconstruction without Ca present [11]. An early STM study [34] which claimed to show a (2×2) surface reconstruction was later demonstrated to be a $(\sqrt{5}\times\sqrt{5})R26.6°$ reconstruction [22,23,35]. Recent STM observations of (2×2) surfaces by Silly et al. [13,14] and Kubo et al. [18] have appeared for samples annealed in ultra-high vacuum (UHV) at 950 °C and 1000 °C, respectively. Kubo et al. [18] proposed a structure consisting of Sr adatoms on a TiO_2-terminated surface; essentially all other works indicate that the surfaces of $SrTiO_3$ are more likely to be TiO_2 rich. Nevertheless, both STM studies showed that the (2×2) surface had a 4-fold symmetry. In 2007, Herger et al. [33] supported the double-layer TiO_2 model using surface X-ray diffraction and showed that there is a coexistence of (2×1), (2×2) and (1×1) reconstructions with a temperature dependence. The (2×2) domains were attributed to the structure which has the lowest surface energy in the DFT study by Warschkow et al. [32], which is usually referred to as the solved (2×2) structure. However, the solved (2×2) has a zigzag surface domain which is unconditionally different from the 4-fold square domain (2×2) obtained by Silly et al. This indicates that two different (2×2) surface structures exist. In this study, new and previously proposed (2×2) models are compared by using STM image simulations to understand the 4-fold square (2×2) surface structure.

* Corresponding author. Tel.: +1 847 491 3267; fax: +1 847 491 7820.
E-mail address: yuyuan-lin@u.northwestern.edu (Y. Lin).

0039-6028/$ – see front matter © 2011 Elsevier B.V. All rights reserved.
doi:10.1016/j.susc.2011.06.001

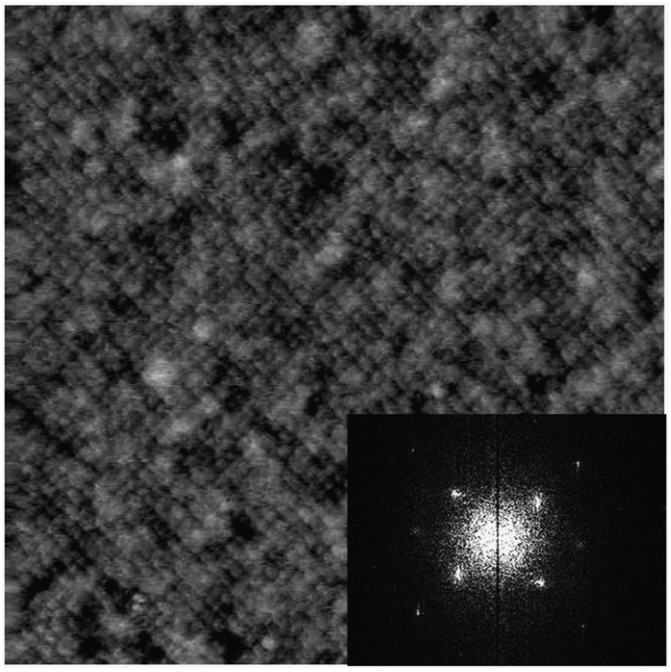

Fig. 1. An STM image with the dimension of 35×35 nm^2 shows a (2×2) surface structure, with sample bias = +0.7 V, tunneling current = 0.1 nA. The inset is the FFT of the STM image. The <001> crystallographic directions run along the diagonals of the image.

The empty states STM image shown in Fig. 1 is from a $SrTiO_3$ (001) epi-polished sample with 0.5 wt.% Nb doping supplied by PI-KEM, U.K. It was chemically etched in a buffered NH_4F–HF solution to remove the polishing damage, and subsequently repeatedly annealed in UHV around 600 °C until the (2×2) reconstruction was formed. The STM experiments were carried out in a JEOL JSTM4500S UHV system with a base pressure of 10^{-10} mbar. Higher-temperature anneals up to 950 °C produced the same (2×2) surface [14]. The (2×2) reconstruction can also be formed by Ar^+ ion bombardment of the surface followed by UHV annealing at 800 °C [13], but this appears to be a more difficult route to generate this surface. A detailed description of the sample preparation and STM imaging conditions can be found in Ref. [14].

Fig. 1 shows a large flat area of (2×2) surface reconstruction. To reveal the detailed structure in the images, a Fourier filtering technique was used to average the image. The power-spectrum of the STM image is inset in Fig. 1. A portion of the filtered image is shown in Fig. 3.

Auger electron spectroscopy (AES) study was carried out to investigate the surface chemistry of samples prepared in this manner. There was no visible signal of Nb up to the detection limit of AES. There were suggestions of slightly reduced oxygen coverage of the (2×2) surface, compared to a UHV-cleaved surface and on this basis the original paper described the surface as reduced. However, the oxygen coverage by AES data is almost the same as that of the $SrTiO_3$ (001)-c(4×2) surface, implying that it is not reduced. We will return to this later.

While it is in principle possible for the reconstruction to be SrO-rich, the only confirmed $SrTiO_3$ (001) surface structures are TiO_2-rich. Moreover, Kawasaki et al. showed that the chemical etching process in weakly acidic NH_4F–HF solution favors the TiO_2-terminated surface by preferentially removing SrO [36], as expected since SrO is a water soluble oxide. Hence four possible surface structures were considered. Three of them are TiO_{2-x}-terminated surface structures of $SrTiO_3$ (001), as shown in (2×2)A, (2×2)B and (2×2)C in Fig. 2. The (2×2)D shown in Fig. 2 is the Sr surface adatom model proposed by Kubo et al. [18]. There is no Nb in any of the DFT models, since the AES study suggests that the Nb presence is negligible in the near-surface region. The (2×2) A and (2×2)C structures in Fig. 2 are double-layer TiO_2-terminated surface models, which were also considered in Warschkow et al.'s work [32]. Although the (2×2)C structure has been structurally solved and has the lowest surface energy among the (2×2) reconstructions according to DFT calculations [32,33], it does not have the 4-fold rotational symmetry found in the STM images. Note that the symmetry differences are over rather large distances, so even accounting for issues with approximations in DFT STM simulations the two will always be very different and we can rule out this structure for *this* set of data. The (2×2)B model, not explored in the aforementioned theoretical study, was considered because of the slight oxygen reduction observed in the original AES study comparing to the UHV cleaved sample, which is also the only qualitative difference with respect to (2×2)A. The (2×2)D model was also chosen as a candidate surface structure because of its correct 4-fold symmetry.

The DFT calculations were performed using the full-electron WIEN2k code [37]. The DFT-optimized lattice parameter $a = 3.944$ Å was used for all the $SrTiO_3$ structures. The TiO_{2-x} terminated surfaces were modeled using a repeated slab configuration, consisting of atomic layers with the following stacking sequence: surface–TiO_2–SrO–TiO_2–SrO–TiO_2–SrO–TiO_2–SrO–TiO_2–SrO–TiO_2–surface. The vacuum spacing between each slab was around 14 Å. The Sr adatom surface was modeled using a similar slab but with one additional layer of both TiO_2 and SrO. The corresponding vacuum spacing was around 13 Å in this case. All atoms were allowed to relax until all forces were below 0.1 eV/Å. Muffin-tin radii of 2.36, 1.70 and 1.20 Bohr were used for Sr, Ti, and O, respectively, as well as a $\min(R_{MT})^*K_{max}$ of 5.5. The PBE version [38] of the generalized gradient approximation for the exchange-correlation energy was employed; tests indicated that for the large potentials used in the STM imaging more accurate methods such as on-site hybrids did not change the images for the experimental resolution. Constant-current STM images were simulated using a modified Tersoff–Hamann approximation [39], considering the states from the Fermi energy to about 1.3 eV above it, after artificially populating these. Also, a weighting term was applied to account for the varying effective tunneling barrier, as well as a blurring effect through a quarter-cosine curve radial convolution feature of radius 2 Å to account for tip-size and thermal effects; the method is described in greater detail in Ref. [40]. The resulting simulated STM images are shown in Fig. 3.

The simulated image from the (2×2)A structure, as shown in Fig. 3, is the closest to the experimental STM image. This is because the row of spots in the filtered image is continuous, as shown in Fig. 3 by red circles. This feature indicates that there is nonzero local DOS (within the imaged energy range) between the large spots in the rows, which is most visible in simulated image from the (2×2)A model. The other models are quantitatively worse fits. As expected, the previously solved (2×2) structure has a zigzag appearance; the difference cannot be corrected by using different simulation parameters (bias voltage, isosurface density).

The main characteristics of the proposed model ((2×2)A in Fig. 2) are the similarity between the structurally solved $SrTiO_3$(001)-c(4×2) [6,17,32] and the one-fold coordinated surface oxygen atoms (O(1) in Fig. 2) at the corner of the surface unit cell. Shifting every second reconstructed cell row in (2×2)A by one bulk lattice constant will result in the solved stable c(4×2) surface. The geometrical similarity may suggest that the (2×2) surface is transformed from the c(4×2) surface by using different sample preparation conditions. The somewhat unusual one-fold coordinated surface oxygen atoms are bonded to the subsurface Ti atoms and form double bonds (denoted Ti═O in the following). The Ti═O has a bond length about 0.3 Å less than that of the typical Ti – O single bond in $SrTiO_3$ bulk structures. The Ti═O is known to exist in Ti containing compounds [7,41–43] and TiO_2 nanoparticles [44,45]. A bond-valence sum [46] analysis shows that the valences for Ti and O atoms of the Ti═O are 3.77 and −1.71 respectively, close to what is expected.

The surface energy calculated for the proposed structure is 1.05 eV per (1×1) unit cell, as determined by subtracting the energy for bulk

$SrTiO_3$ and TiO_2 from the total energy. This is comparable to other structures with the same stoichiometry modeled using the same DFT calculation parameters. Although the (2×2)A surface is not the lowest energy structure, all other competitors such as the c(4×2) have drastically different symmetries. Exactly why it forms we leave as an open question for future work; clearly it is not just thermodynamics but kinetics also play a critical role a point which is starting to be clearer for oxide surfaces. It is worth remarking that two different reconstructions with the same stoichiometry and periodicity is possible; our present report of the (2×2)A does not contradict the identification by Herger et al. [33] of the (2×2)C.

Usually, annealing in UHV results in a slight reduction of the oxide surface. However, our model of the (2×2)A is fully oxidized. In the earlier paper on the (2×2) reconstruction [14] it was stated that Auger

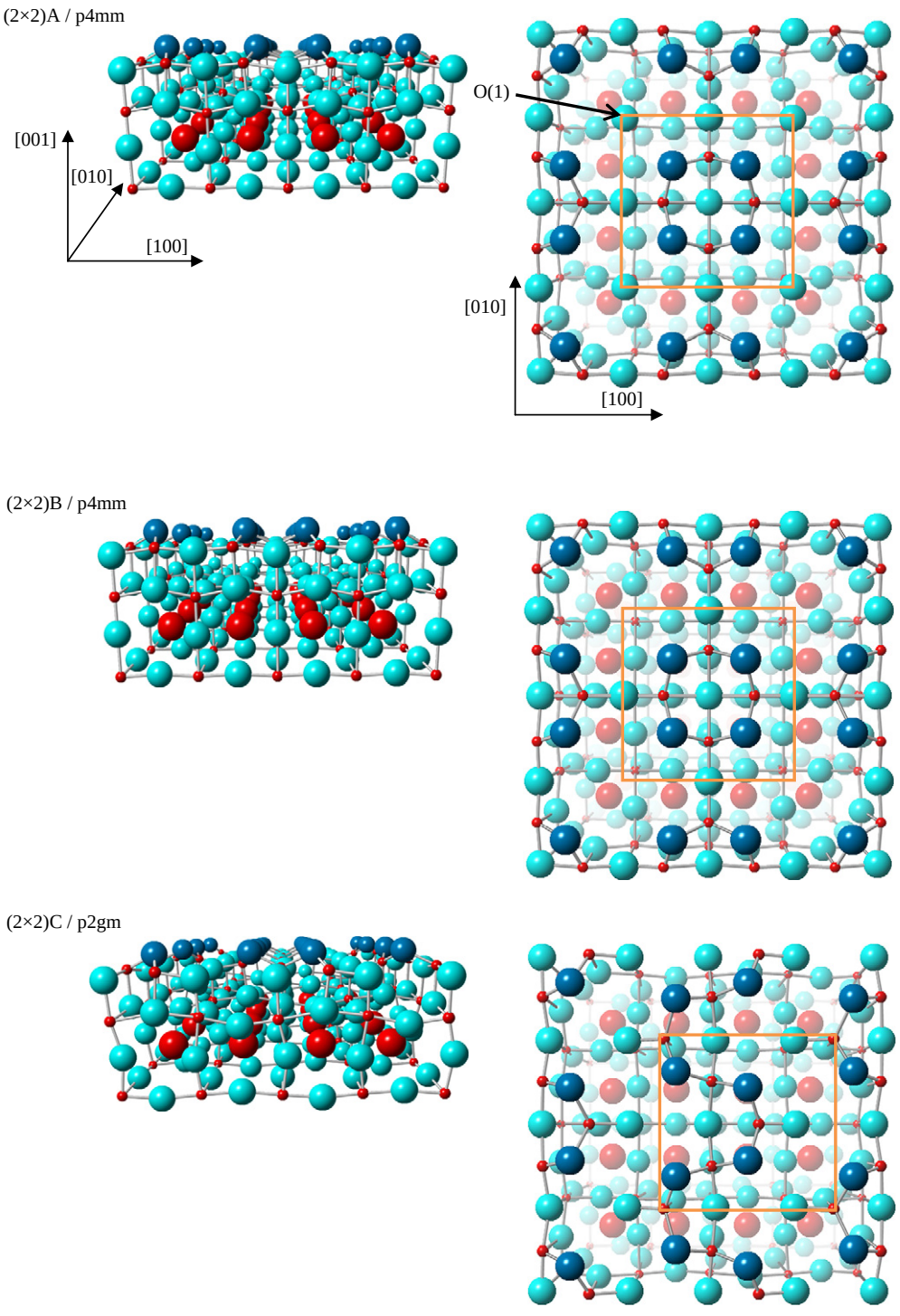

Fig. 2. Side and top views of four possible (2×2) surface reconstructions. Ti and Sr atoms are represented by small and big red spheres respectively. O-atoms are colored light blue and dark blue. The dark blue O-atoms are "floating" atoms without bonding to the subsurface. The unit cell for each model is indicated by an orange square. (2×2)A and (2×2)C are double-layer TiO_2-terminated surfaces and only different by the distribution of atoms. (2×2)A and (2×2)B share a same symmetry but the latter one has no oxygen at the corner of the unit cell. (2×2)D shows Sr adatom reconstruction model on a TiO_2 terminated sub-surface.

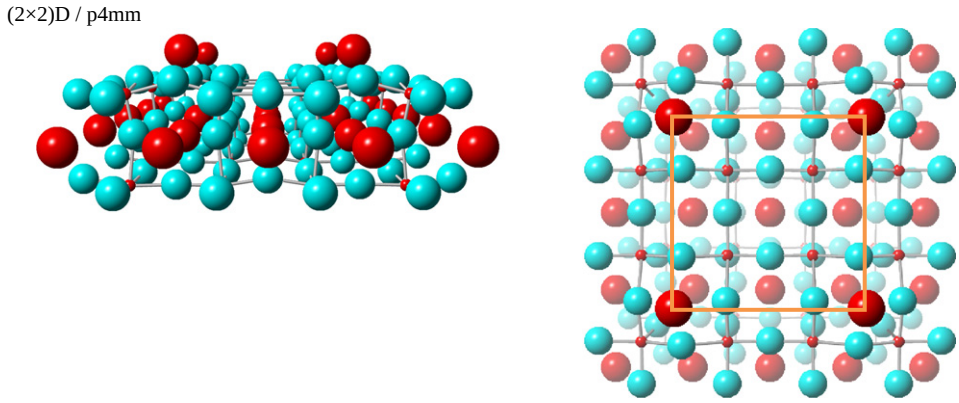

Fig. 2 (*continued*).

electron spectroscopy showed a reduction of the oxygen signal relative to a UHV cleaved sample. As mentioned above, the oxygen signal is comparable with that found for the $SrTiO_3$ (001)-c(4×2) which has a double-layer TiO_2 terminated surface and is full oxidized. Our subsequent experiments have shown that the oxygen peak height reduction is between 3 and 7%, but that there is no discernible titanium enrichment. The origin of the oxygen peak height reduction could be due to any number of factors that are not related to the structure of the surface reconstruction. The factors are: the UHV cleaved surface is not necessarily a good reference of stoichiometry as it can readily adsorb water and other oxygen containing molecules; the oxygen deficiency is due to randomly distributed oxygen vacancies; different reconstructions result in different shadowing and Auger electron diffraction effects that affect the oxygen peak height.

In conclusion, everything points to the (2×2) p4mm surface being the structure which had been previously proposed [32]. The surface is a double-layer TiO_2-terminated structure with a p4mm space symmetry and is not oxygen reduced.

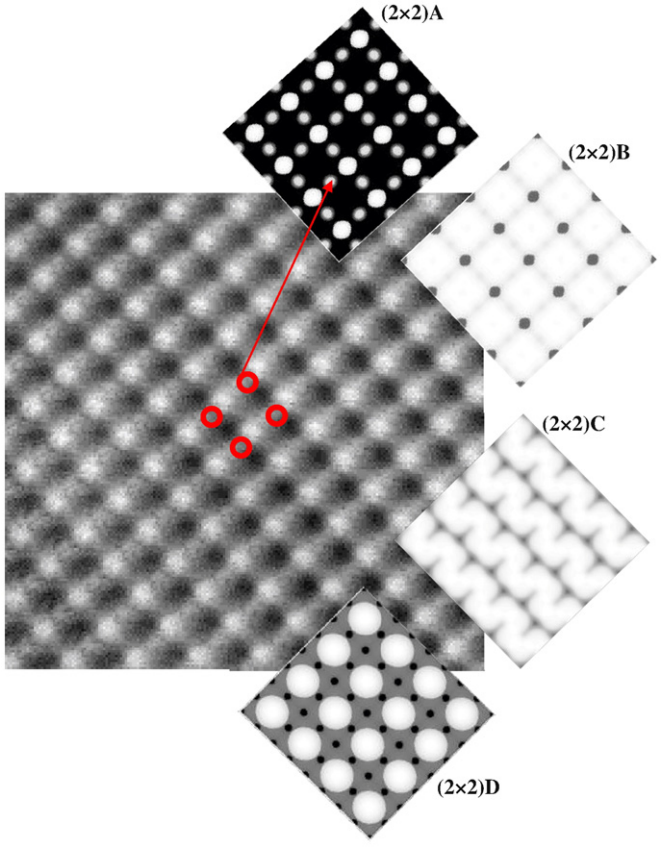

Fig. 3. The Fourier-filtered STM image with DFT-simulated images based on four different surface models on the right side. The red circles and arrow indicate the non-zero local DOS between the bright large spots, which is more compatible with the feature in the image simulated by the (2×2)A model.

Acknowledgments

We acknowledge funding from the Northwestern University Institute for Catalysis in Energy Processes (ICEP) on grant number DOE DE-FG02-03-ER15457 (YL) and DOE grant number DOE DE-FG02-01ER45945 (AEB).

Appendix A. Supplementary data

Supplementary data to this article can be found online at doi:10.1016/j.susc.2011.06.001.

References

[1] J.G. Mavroides, J.A. Kafalas, D.F. Kolesar, Appl. Phys. Lett. 28 (1976) 241.
[2] M. Kawasaki, K. Takahashi, T. Maeda, R. Tsuchiya, M. Shinohara, O. Ishiyama, T. Yonezawa, M. Yoshimoto, H. Koinuma, Science 266 (1994) 1540.
[3] F.A. Rabuffetti, H.-S. Kim, J.A. Enterkin, Y. Wang, C.H. Lanier, L.D. Marks, K.R. Poeppelmeier, P.C. Stair, Chem. Mater. 20 (2008) 5628.
[4] J.A. Enterkin, K.R. Poeppelmeier, L.D. Marks, Nano Lett. 11 (2011) 993.
[5] B. Cord, R. Courths, Surf. Sci. 162 (1985) 34.
[6] M.R. Castell, Surf. Sci. 505 (2002) 1.
[7] N. Erdman, K.R. Poeppelmeier, M. Asta, O. Warschkow, D.E. Ellis, L.D. Marks, Nature 419 (2002) 55.
[8] K. Johnston, M.R. Castell, A.T. Paxton, M.W. Finnis, Phys. Rev. B 70 (2004) 085415.
[9] J.E.T. Andersen, P.J. Moller, Appl. Phys. Lett. 56 (1990) 1847.
[10] Q.D. Jiang, J. Zegenhagen, Surf. Sci. 338 (1995) L882.
[11] P.J. Møller, S.A. Komolov, E.F. Lazneva, Surf. Sci. 425 (1999) 15.
[12] T. Nishimura, A. Ikeda, H. Namba, T. Morishita, Y. Kido, Surf. Sci. 421 (1999) 273.
[13] F. Silly, M.R. Castell, Appl. Phys. Lett. 87 (2005) 053106.
[14] F. Silly, D.T. Newell, M.R. Castell, Surf. Sci. 600 (2006) 219.
[15] T. Ohsawa, K. Iwaya, R. Shimizu, T. Hashizume, T. Hitosugi, J. Appl. Phys. 108 (2010) 073710.
[16] Q.D. Jiang, J. Zegenhagen, Surf. Sci. 425 (1999) 343.
[17] N. Erdman, O. Warschkow, M. Asta, K.R. Poeppelmeier, D.E. Ellis, L.D. Marks, J. Am. Chem. Soc. 125 (2003) 10050.
[18] T. Kubo, H. Nozoye, Surf. Sci. 542 (2003) 177.
[19] C.H. Lanier, A. van de Walle, N. Erdman, E. Landree, O. Warschkow, A. Kazimirov, K.R. Poeppelmeier, J. Zegenhagen, M. Asta, L.D. Marks, Phys. Rev. B 76 (2007) 045421.
[20] H. Tanaka, T. Matsumoto, T. Kawai, S. Kawai, Surf. Sci. 318 (1994) 29.
[21] M.S. Martín González, M.H. Aguirre, E. Morán, M.Á. Alario-Franco, V. Perez-Dieste, J. Avila, M.C. Asensio, Solid State Sci. 2 (2000) 519.
[22] T. Kubo, H. Nozoye, Phys. Rev. Lett. 86 (2001) 1801.
[23] D.T. Newell, A. Harrison, F. Silly, M.R. Castell, Phys. Rev. B 75 (2007) 205429.
[24] M. Naito, H. Sato, Phys. C 229 (1994) 1.
[25] D.M. Kienzle, A.E. Becerra-Toledo, L.D. Marks, Phys. Rev. Lett. 106 (2011) 176102.

[26] M.R. Castell, Surf. Sci. 516 (2002) 33.
[27] D.S. Deak, F. Silly, D.T. Newell, M.R. Castell, J. Phys. Chem. B 110 (2006) 9246.
[28] D.S. Deak, F. Silly, K. Porfyrakis, M.R. Castell, J. Am. Chem. Soc. 128 (2006) 13976.
[29] H.L. Marsh, D.S. Deak, F. Silly, A.I. Kirkland, M.R. Castell, Nanotechnology 17 (2006) 3543.
[30] D.S. Deak, F. Silly, K. Porfyrakis, M.R. Castell, Nanotechnology 18 (2007) 075301.
[31] C. Lu, E. Zhu, Y. Liu, Z. Liu, Y. Lu, J. He, D. Yu, Y. Tian, B. Xu, J. Phys. Chem. C 114 (2010) 3416.
[32] O. Warschkow, M. Asta, N. Erdman, K.R. Poeppelmeier, D.E. Ellis, L.D. Marks, Surf. Sci. 573 (2004) 446.
[33] R. Herger, P.R. Willmott, O. Bunk, C.M. Schlepütz, B.D. Patterson, B. Delley, Phys. Rev. Lett. 98 (2007) 076102.
[34] T. Matsumoto, H. Tanaka, T. Kawai, S. Kawai, Surf. Sci. 278 (1992) L153.
[35] T. Matsumoto, H. Tanaka, K. Kouguchi, T. Kawai, S. Kawai, Surf. Sci. 312 (1994) 21.
[36] M. Kawasaki, A. Ohtomo, T. Arakane, K. Takahashi, M. Yoshimoto, H. Koinuma, Appl. Surf. Sci. 107 (1996) 102.
[37] P. Blaha, et al., WIEN2k An augmented Plane Wave Plus Local Orbitals Program for Calculating Crystal Properties, Technical Univ, Vienna, 2001.
[38] J.P. Perdew, K. Burke, M. Ernzerhof, Phys. Rev. Lett. 77 (1996) 3865.
[39] J. Tersoff, D.R. Hamann, Phys. Rev. B 31 (1985) 805.
[40] M.S.J. Marshall, A.E. Becerra-Toledo, M.R. Castell, L.D. Marks, In Preparation, (2011).
[41] M.A. Roberts, G. Sankar, J.M. Thomas, R.H. Jones, H. Du, J. Chen, W. Pang, R. Xu, Nature 381 (1996) 401.
[42] F. Farges, G.E. Brown, J.J. Rehr, Phys. Rev. B 56 (1997) 1809.
[43] T.J. Beck, A. Klust, M. Batzill, U. Diebold, C. Di Valentin, A. Selloni, Phys. Rev. Lett. 93 (2004) 036104.
[44] T. Rajh, J.M. Nedeljkovic, L.X. Chen, O. Poluektov, M.C. Thurnauer, J. Phys. Chem. B 103 (1999) 3515.
[45] P.C. Redfern, P. Zapol, L.A. Curtiss, T. Rajh, M.C. Thurnauer, J. Phys. Chem. B 107 (2003) 11419.
[46] I.D. Brown, D. Altermatt, Acta Crystallogr. B 41 (1985) 244.